Electronic Supplementary Material (ESI) for Molecular Omics.

Supplementary data

Mycobacterium bovis BCG infection alters the macrophage N-glycome

Clément Delannoy, Chin Huang, Bernadette Coddeville, Jian-You Chen, Dounia Mouajjah, Sophie Groux-Degroote, Anne Hardhuin-Lepers, Kay-Hooi Khoo, Yann Guerardel, Elisabeth Elass-Rochard

SIFigure. 1 Inflammatory status of cells after stimulation . Differentiated THP-1 cells or MDM were activated by infection with *M. bovis* BCG or by incubation with the lipopeptide PAM_3LP_{19}. After 72h, the expression levels of ICAM-1, CD40 and CD80 antigens at the cell surface of stimulated THP-1 cells (A) and MDM (B) cells (peak 1) were determined by flow cytometry, using specific antibodies and then compared with untreated cells (grey peak 2). The non-specific binding of antibodies to stimulated cells were evaluated with isotype control antibodies (peak 3). Results are shown as linear-log scale fluorescence histograms. The data are from one representative experiment of three independent experiments with similar results. (C) Culture supernatants were collected after 8 or 24 h and assayed by ELISA for TNF-α and IL-1β secretion, respectively. Similar experiments were performed after incubation of PMA THP-1 cells with Pam_3LP_{19}. Data are expressed as means ± SD of triplicates and are representative from three independent experiments. Statistical analyses were performed by using student *t* test. (*** *p* values < 0.001).

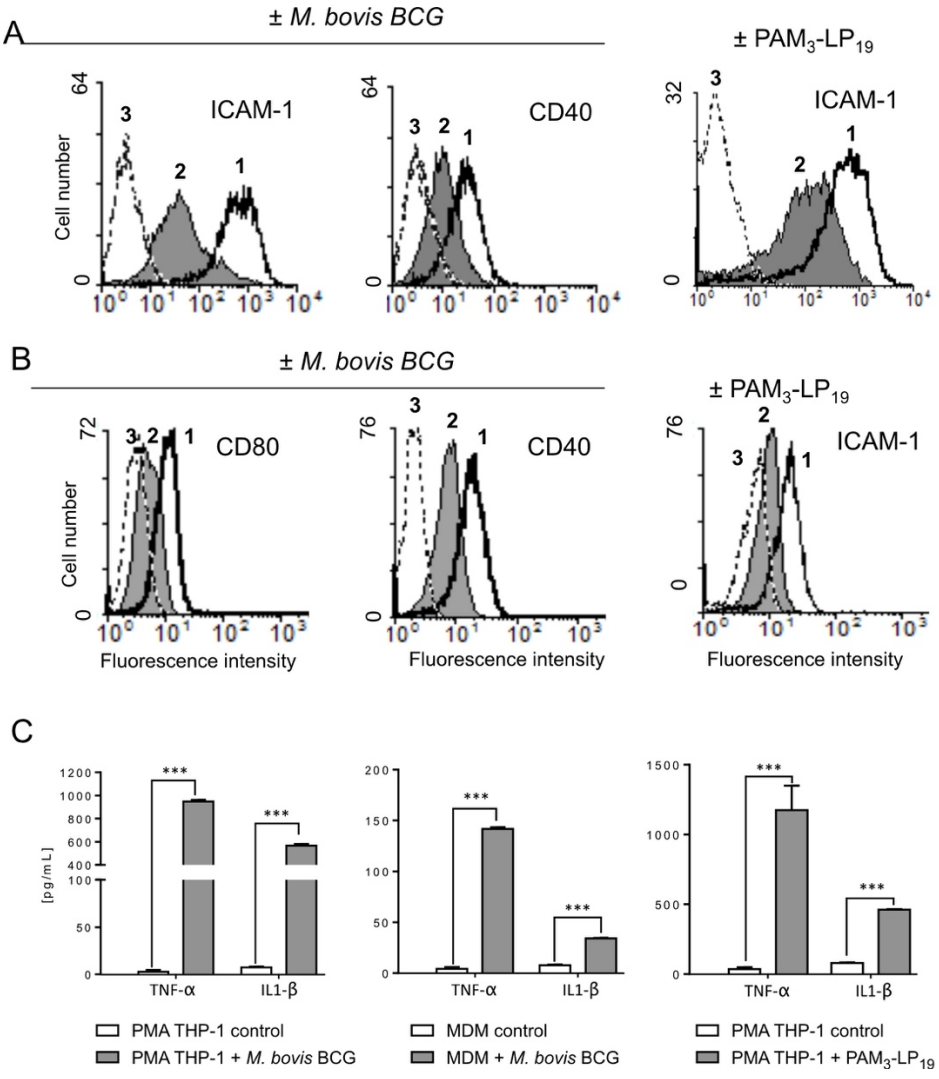

SIFigure 2: Comparative MALDI-MS analyses of glycosphingolipids extracted from THP-1. MALDI-MS profiles of permethylated glycosphingolipids purified from PMA-differentiated THP-1 cells (A) before and (B) after BCG infection. (C) MALDI-TOF/TOF MS/MS sequencing of GSL at *m/z* 1460.

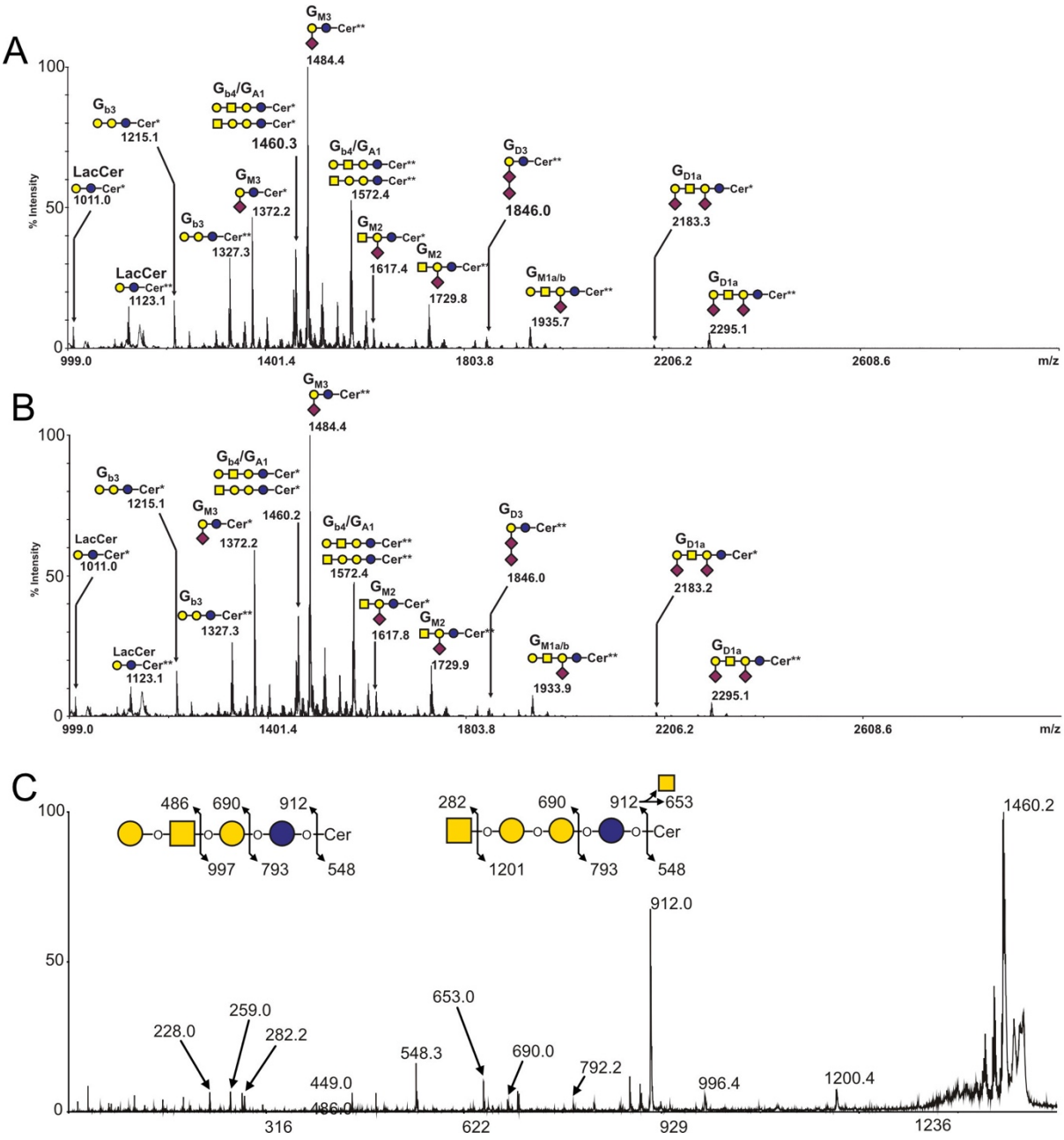

SIFigure 3: Comparative MALDI-MS analyses of glycosphingolipids extracted from MDM. MALDI-MS profiles of permethylated glycosphingolipids purified from MDM cells cells (A) before and (B) after BCG infection.

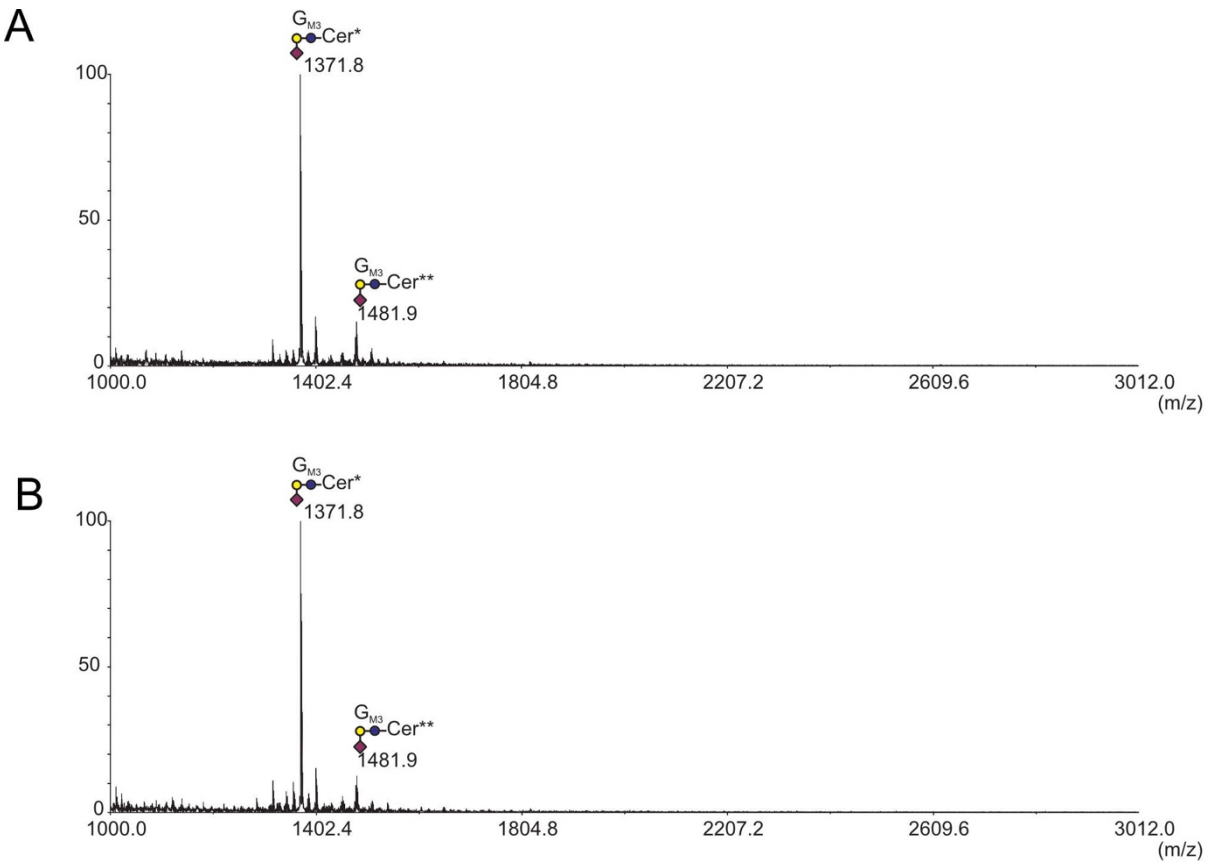

SIFigure 4. MALDI-MS analyses of N-glycans from MDM without (upper panels) and with (lower panels) BCG treatment. The released N-glycans were reduced and permethylated directly (**A**) or additionally subjected to sialyl linkage specific dimethylamidation prior to permethylation (**B**). Only part of the entire mass range acquired was shown here to highlight the difucosylated complex type N-glycans. The spectra of dimethylamidated samples (**B**) were more complex due to conversion of sialylated peaks to multiple +13 u peaks, which corresponds also to the mass difference between 2 Fuc and 1 NeuAc, as well as overlapping partially with under methylated peaks (-14 u). Glycosyl composition assignment here was based on the detected mass values for the $[M+Na]^+$ molecular ions and annotated using the standard Symbol Nomenclature for Glycan system (Varki et al. 2015). The first Fuc is depicted as core Fuc on a common trimannosyl core for all while the second Fuc is attributed to peripheral antennary Fuc based on additional LC-MS/MS analysis. In source prompt fragmentation produced several characteristic oxonium ions, which allows a rapid mapping and inference of the various terminal glycotopes (see SIFigure 5 and SIFigure 7).

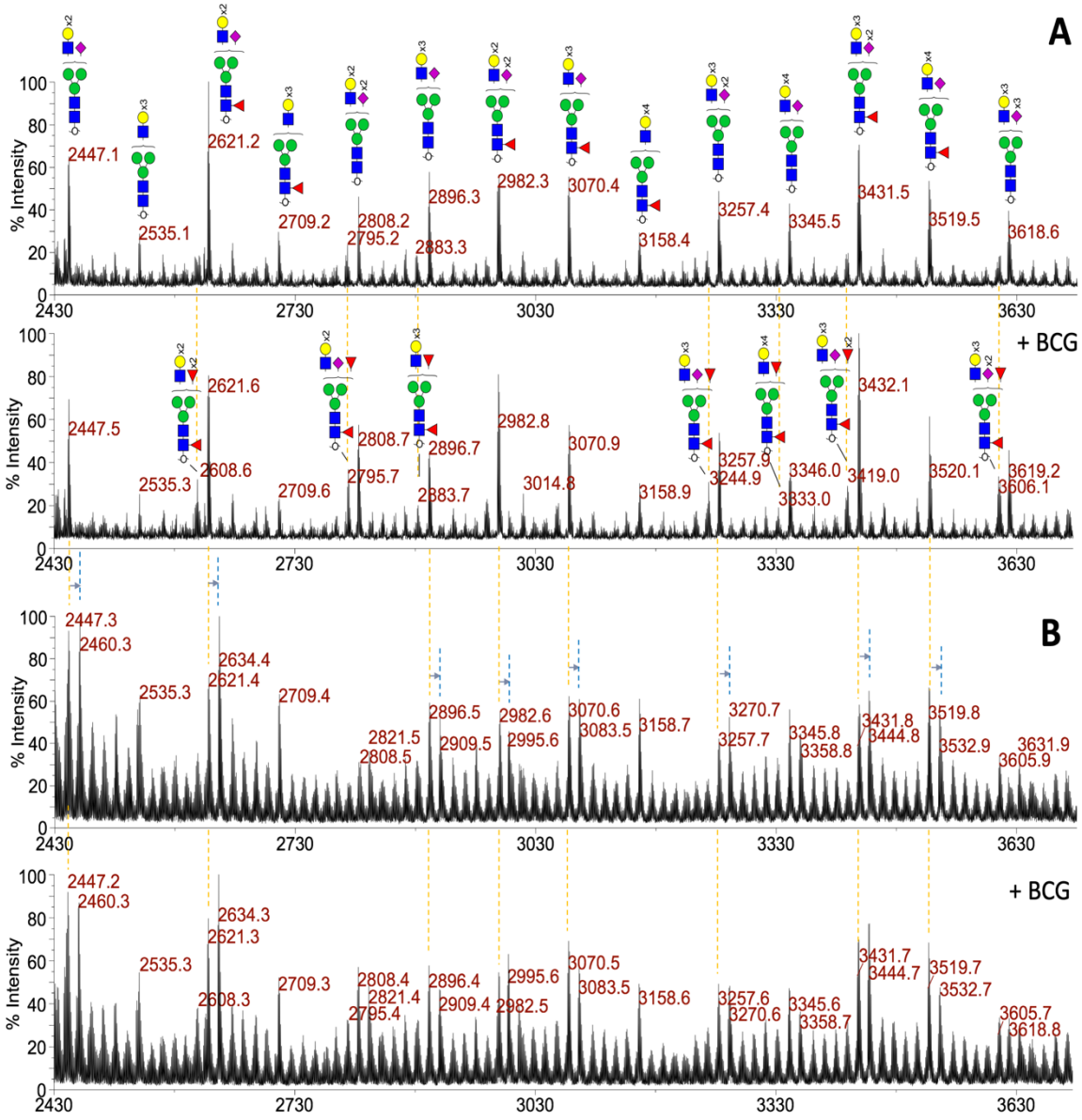
A
% Intensity
2447.1
2535.1
2621.2
2709.2
2795.2
2808.2
2883.3
2896.3
2982.3
3070.4
3158.4
3257.4
3345.5
3431.5
3519.5
3618.6
+ BCG
2447.5
2535.3
2608.6
2621.6
2709.6
2795.7
2808.7
2883.7
2896.7
2982.8
3014.8
3070.9
3158.9
3244.9
3257.9
3333.0
3346.0
3419.0
3432.1
3520.1
3606.1
3619.2
B
2447.3
2460.3
2535.3
2621.4
2634.4
2709.4
2808.5
2821.5
2896.5
2909.5
2982.6
2995.6
3070.6
3083.5
3158.7
3257.7
3270.7
3345.8
3358.8
3431.8
3444.8
3519.8
3532.9
3605.9
3631.9
+ BCG
2447.2
2460.3
2535.3
2608.3
2621.3
2634.3
2709.3
2795.4
2808.4
2821.4
2896.4
2909.4
2982.5
2995.6
3070.5
3083.5
3158.6
3257.6
3270.6
3345.6
3358.7
3431.7
3444.7
3519.7
3532.7
3605.7
3618.8
2430
2730
3030
3330
3630

SIFigure 5. The low mass region of the MALDI-MS profiles of dimethylamidated permethylated N-glycans from MDM without (A) and with (B) BCG treatment. The various in source-produced oxonium ions are as annotated, with the ion at *m/z* 638 corresponding to Fuc(HexHexNAc) only detected in BCG treated sample. The relative ratio of *m/z* 825/838 is a good indicator of the relative total amount α2-3 and 2-6-sialylation but that of *m/z* 376/389 is not, due to preferential cleavages of dimethylamidated sialic acid residues.

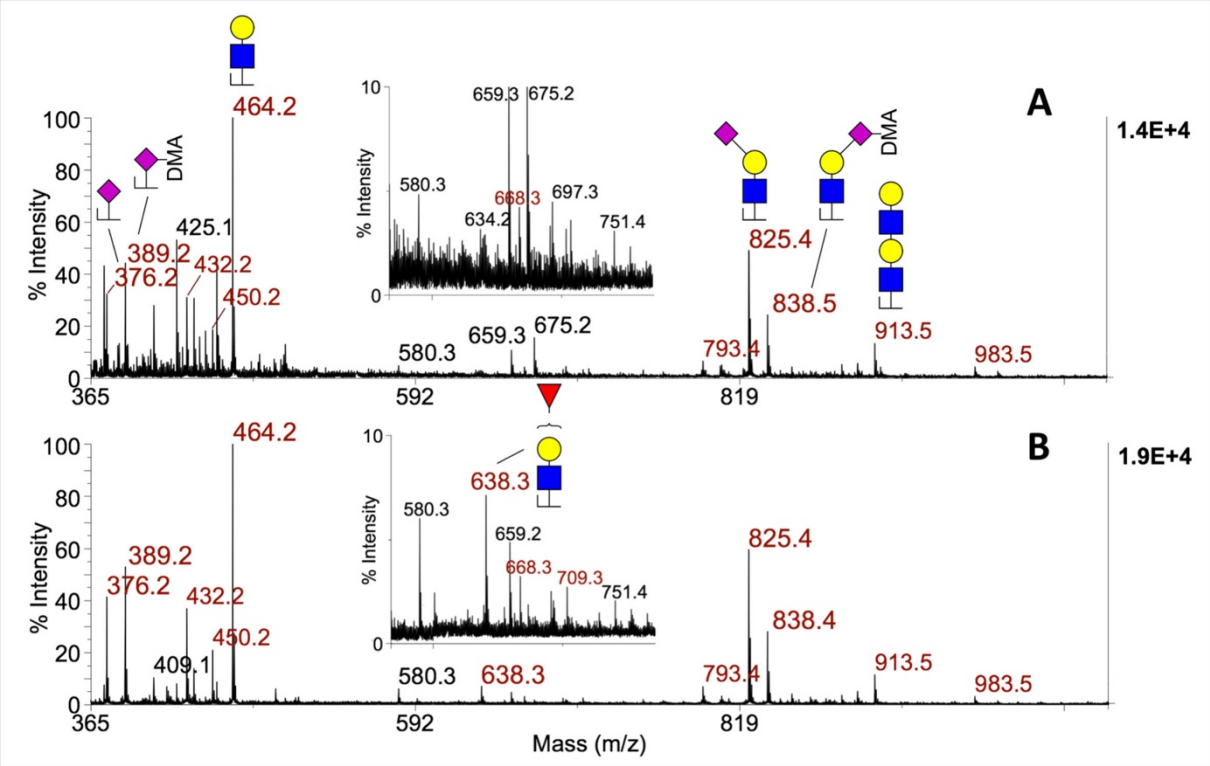

SIFigure 6: **MALDI-QIT-TOF MS/MS sequencing of fucosylated permethylated *N*-glycan at *m/z* 2605**. Fragmentation pattern establishes the presence of at least two glycoforms differing by the substitution position of fucose residue either on chitobiose core or on LacNac antenna. Both glycoforms could be individually analyzed in reduced form by nanoESI HCD MS/MS, as shown in SIFigure 7 (upper panel).

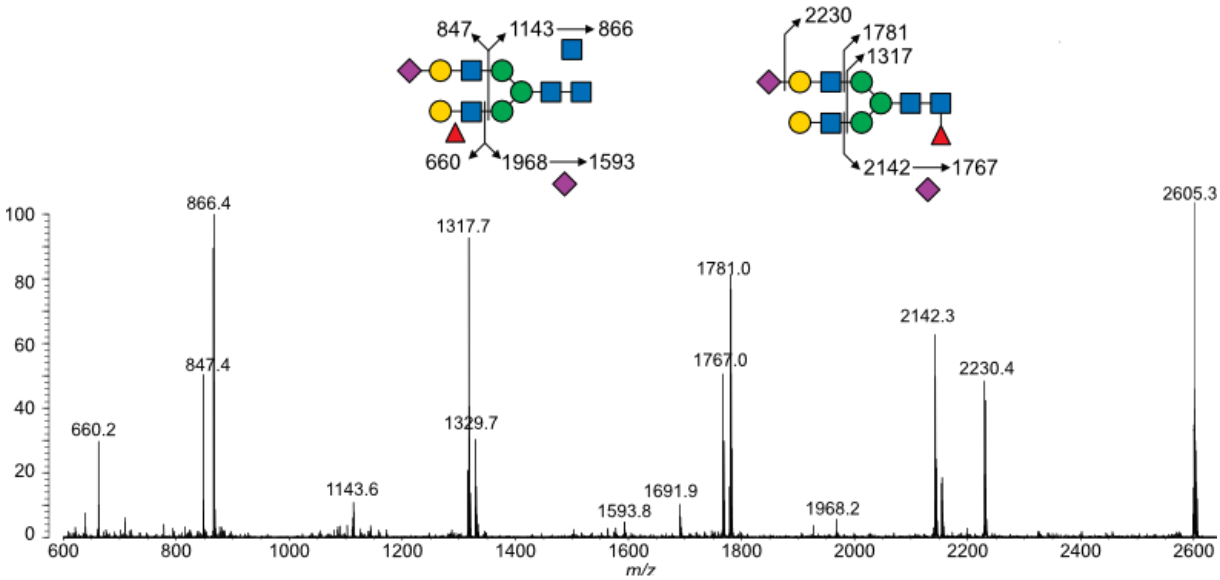

***SIFigure 7*. Representative single scan nanoESI HCD MS/MS spectra acquired on the reduced, permethylated N-glycans derived from MDM+BCG.** The precursors were either doubly or triply protonated, with their m/z indicated on respective spectral header. Not all ions were annotated. The important diagnostic ions are the oxonium ions at m/z 825, 638 and 464, corresponding to $NeuAcHexHexNAc^+$, $FucHexHexNAc^+$, and $HexHexNAc^+$, respectively. Ion at *m/z* 793 indicates a sialyl Hex-4HexNAc, the HeNAc of which is not substituted at position 3. *M/z* 432 could be derived from either *m/z* 464 or 638 after elimination of a MeOH or Fuc from position 3, respectively. The absence of *m/z* 228 further confirm a type 2 LacNAc or LeX unit. The Y1 ion at m/z 468, where present, identifies a core fucosylated HexNAcitol.

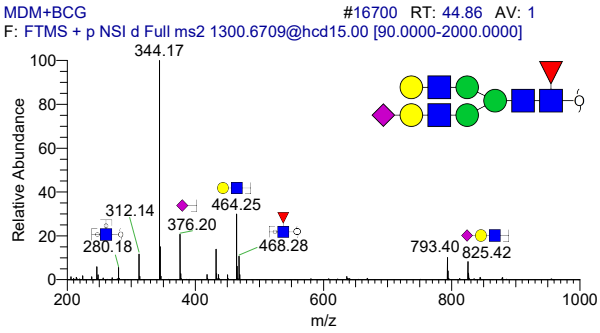
MDM+BCG #16700 RT: 44.86 AV: 1
F: FTMS + p NSI d Full ms2 1300.6709@hcd15.00 [90.0000-2000.0000]
344.17
312.14
376.20
464.25
280.18
468.28
793.40
825.42
Relative Abundance
m/z

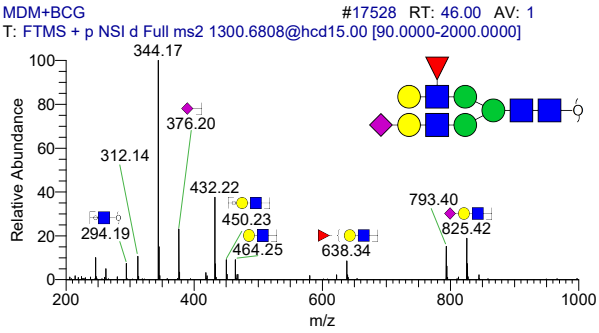
MDM+BCG #17528 RT: 46.00 AV: 1
T: FTMS + p NSI d Full ms2 1300.6808@hcd15.00 [90.0000-2000.0000]
344.17
376.20
312.14
432.22
450.23
294.19
464.25
638.34
793.40
825.42
Relative Abundance
m/z

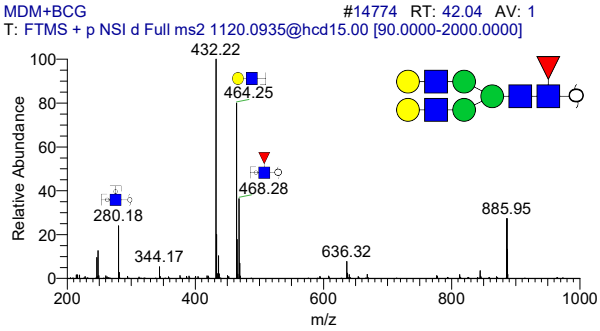
MDM+BCG #14774 RT: 42.04 AV: 1
T: FTMS + p NSI d Full ms2 1120.0935@hcd15.00 [90.0000-2000.0000]
432.22
464.25
468.28
280.18
885.95
344.17
636.32
Relative Abundance
m/z

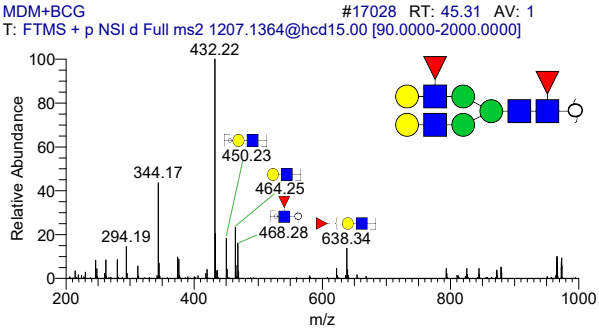
MDM+BCG #17028 RT: 45.31 AV: 1
T: FTMS + p NSI d Full ms2 1207.1364@hcd15.00 [90.0000-2000.0000]
432.22
450.23
344.17
464.25
294.19
468.28
638.34
Relative Abundance
m/z

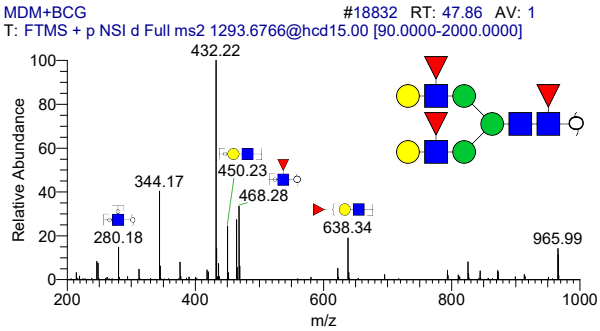
MDM+BCG #18832 RT: 47.86 AV: 1
T: FTMS + p NSI d Full ms2 1293.6766@hcd15.00 [90.0000-2000.0000]
432.22
450.23
344.17
468.28
638.34
280.18
965.99
Relative Abundance
m/z

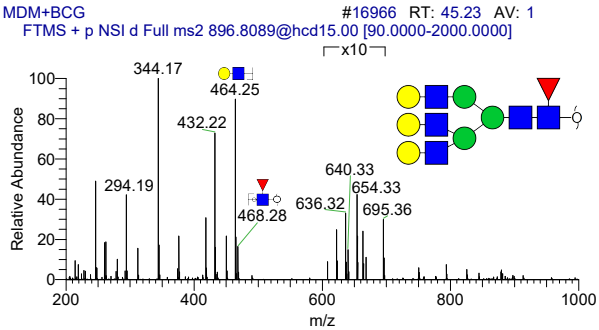
MDM+BCG #16966 RT: 45.23 AV: 1
FTMS + p NSI d Full ms2 896.8089@hcd15.00 [90.0000-2000.0000]
x10
344.17
464.25
432.22
294.19
640.33
654.33
636.32
468.28
695.36
Relative Abundance
m/z

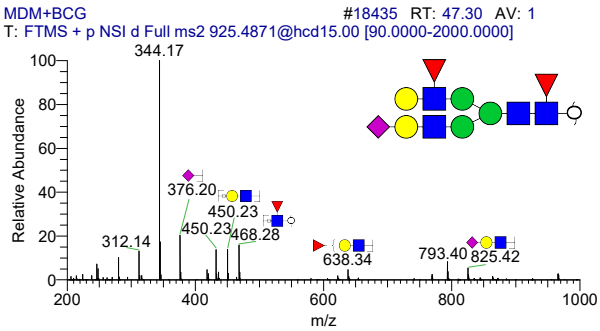
MDM+BCG #18435 RT: 47.30 AV: 1
T: FTMS + p NSI d Full ms2 925.4871@hcd15.00 [90.0000-2000.0000]
344.17
376.20
450.23
450.23
468.28
312.14
638.34
793.40
825.42
Relative Abundance
m/z

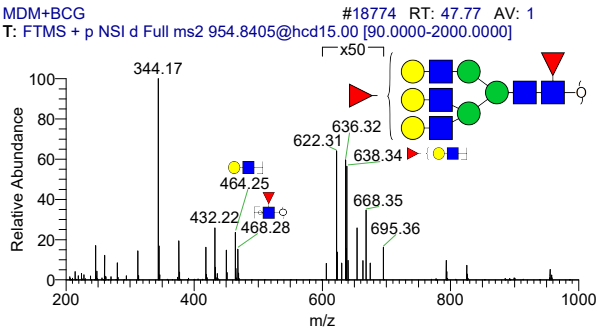
MDM+BCG #18774 RT: 47.77 AV: 1
T: FTMS + p NSI d Full ms2 954.8405@hcd15.00 [90.0000-2000.0000]
x50
344.17
636.32
622.31
638.34
464.25
668.35
432.22
468.28
695.36
Relative Abundance
m/z

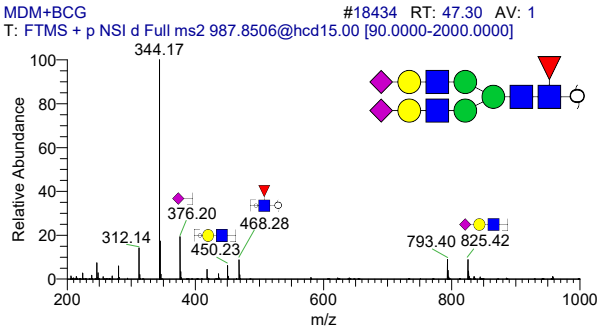
MDM+BCG #18434 RT: 47.30 AV: 1
T: FTMS + p NSI d Full ms2 987.8506@hcd15.00 [90.0000-2000.0000]
344.17
376.20
468.28
312.14
450.23
793.40
825.42
Relative Abundance
m/z

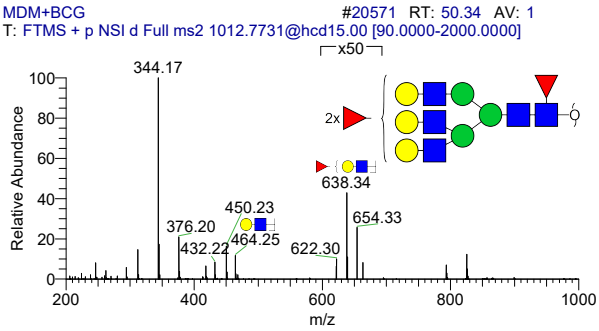
MDM+BCG #20571 RT: 50.34 AV: 1
T: FTMS + p NSI d Full ms2 1012.7731@hcd15.00 [90.0000-2000.0000]
x50
344.17
2x
638.34
450.23
654.33
376.20
464.25
432.22
622.30
Relative Abundance
m/z

SITable 1: Assignment of molecular ions ([M + Na]$^+$) observed in MALDI-MS profiles of permethylated N-glycans of infected and untreated macrophage THP-1 cells

	Permethylated mono-isotopic molecular masses				
	Theo.	**Obs.**	**Composition**	**THP1 cells**	**MDM cells**
High mannose	1579,78	1579.8	$Hex_5HexNAc_2$	✓	✓
	1783,88	1783.9	$Hex_6HexNAc_2$	✓	✓
	1987,98	1988.0	$Hex_7HexNAc_2$	✓	✓
	2192,08	2192.1	$Hex_8HexNAc_2$	✓	✓
	2396,18	2396.2	$Hex_9HexNAc_2$	✓	✓
Bi-LacNac	1590,80	1590.8	$Fuc_1Hex_3HexNAc_3$	✓	✓
	1620,81	1620.8	$Hex_4HexNAc_3$	✓	✓
	1835,92	1835.9	$Fuc_1Hex_3HexNAc_4$	✓	✓
	2070,04	2070.0	$Hex_5HexNAc_4$	✓	✓
	2081,05	2081.1	$Fuc_1Hex_3HexNAc_5$	✓	-
	2244,12	2244.1	$Fuc_1Hex_5HexNAc_4$	✓	✓
	2418,21	2418.2	$Fuc_2Hex_5HexNAc_4$	✓	-
	2431,21	2431.2	$NeuAc_1Hex_5HexNAc_4$	✓	✓
	2592,30	2592.3	$Fuc_3Hex_5HexNAc_4$	✓	✓
	2605,30	2605.3	$NeuAc_1Fuc_1Hex_5HexNAc_4$	✓	✓
	2779,39	2779.4	$NeuAc_1Fuc_2Hex_5HexNAc_4$	✓	✓
	2792,38	2792.4	$NeuAc_2Hex_5HexNAc_4$	✓	✓
	2953,48	2953.5	$NeuAc_1Fuc_3Hex_5HexNAc_4$	-	✓
	2966,47	2966.5	$NeuAc_2Fuc_1Hex_5HexNAc_4$	✓	✓
	3314,65	3314.7	$NeuAc_2Fuc_3Hex_5HexNAc_4$	✓	✓
Tri-LacNAc	2519,26	2519.3	$Hex_6HexNAc_5$	✓	✓
	2693,35	2692.3	$Fuc_1Hex_6HexNAc_5$	✓	✓
	2867,44	2867.4	$Fuc_2Hex_6HexNAc_5$	✓	✓
	2880,44	2880.4	$NeuAc_1Hex_6HexNAc_5$	✓	✓
	3054,52	3054.5	$NeuAc_1Fuc_1Hex_6HexNAc_5$	-	✓
	3228,61	3228.6	$NeuAc_1Fuc_2Hex_6HexNAc_5$	✓	✓
	3241,61	3241.6	$NeuAc_2Hex_6HexNAc_5$	✓	✓
	3415,70	3415.7	$NeuAc_2Fuc_1Hex_6HexNAc_5$	✓	✓
	3589,79	3589.8	$NeuAc_2Fuc_2Hex_6HexNAc_5$	✓	✓
	3602,78	3602.8	$NeuAc_3Hex_6HexNAc_5$	✓	✓
	3776,87	3776.9	$NeuAc_3Fuc_1Hex_6HexNAc_5$	✓	✓
Tetra-LacNAc	3142,58	3142.6	$Fuc_1Hex_7HexNAc_6$	✓	✓
	3316,67	3316.7	$Fuc_2Hex_7HexNAc_6$	✓	✓
	3329,66	3329.7	$NeuAc_1Hex_7HexNAc_6$	✓	✓
	3503,75	3503.8	$NeuAc_1Fuc_1Hex_7HexNAc_6$	✓	✓
	3677,84	3677.9	$NeuAc_1Fuc_2Hex_7HexNAc_6$	✓	✓
	3690,83	3690.8	$NeuAc_2Hex_7HexNAc_6$	✓	✓
	3864,92	3864.9	$NeuAc_2Fuc_1Hex_7HexNAc_6$	✓	✓

	4039,01	4039.0	$NeuAc_2Fuc_2Hex_7HexNAc_6$	✓	-
	4226,10	4226.1	$NeuAc_3Fuc_1Hex_7HexNAc_6$	✓	-
	4400,19	4400.2	$NeuAc_3Fuc_2Hex_7HexNAc_6$	✓	-
	4587,27	4587.3	$NeuAc_4Fuc_1Hex_7HexNAc_6$	✓	-
	4761,36	4761.4	$NeuAc_4Fuc_2Hex_7HexNAc_6$	✓	-
Penta-LacNAc	3591,80	3591.8	$Fuc_1Hex_8HexNAc_7$	✓	✓
	3952,98	3953.0	$NeuAc_1Fuc_1Hex_8HexNAc_7$	✓	✓
	4127,07	4127.1	$NeuAc_1Fuc_2Hex_8HexNAc_7$	✓	-
	4314,15	4314.2	$NeuAc_2Fuc_1Hex_8HexNAc_7$	✓	-
	4488,24	4488.2	$NeuAc_2Fuc_2Hex_8HexNAc_7$	✓	-
	4675,32	4675.3	$NeuAc_3Fuc_1Hex_8HexNAc_7$	✓	-
	4849,41	4849.3	$NeuAc_3Fuc_2Hex_8HexNAc_7$	✓	-